RESEARCH PAPER

PCCP
www.rsc.org/pccp

Femtosecond fluorescence up-conversion spectroscopy of a rotation-restricted azobenzene after excitation to the S_1 state†

T. Pancur,[a] F. Renth,*[a] F. Temps,*[a] B. Harbaum,[b] A. Krüger,[b] R. Herges[b] and Chr. Näther[c]

[a] *Institut für Physikalische Chemie, Christian-Albrechts-Universität zu Kiel, Ludewig-Meyn-Str. 8, D-24098 Kiel, Germany. E-mail: renth@phc.uni-kiel.de, temps@phc.uni-kiel.de*
[b] *Institut für Organische Chemie, Christian-Albrechts-Universität zu Kiel, Otto-Hahn-Platz 3, D-24098 Kiel, Germany*
[c] *Institut für Anorganische Chemie, Christian-Albrechts-Universität zu Kiel, Otto-Hahn-Platz 6–7, D-24098 Kiel, Germany*

Received 23rd December 2004, Accepted 24th March 2005
First published as an Advance Article on the web 11th April 2005

Femtosecond time-resolved fluorescence up-conversion spectroscopy has been used in a study of the photo-induced isomerization reactions of a rotation-restricted *trans*-azobenzene (*trans*-AB) derivative capped by a crown ether (**1**), a chemically similar open derivative (**2**), and unsubstituted *trans*-AB (**3**) after excitation to the S_1 ($n\pi^*$) state at $\lambda = 475$ nm in dioxane solution. The observed biexponential temporal fluorescence profiles for **1** and **2** were almost indistinguishable within experimental error. The fitted fast fluorescence decay times ($\pm 2\sigma$) for the two compounds were τ_1 (**1**) = (0.79 ± 0.20) and τ_1 (**2**) = (1.05 ± 0.20) ps, compared to τ_1 (**3**) = (0.37 ± 0.06) ps. The second decay components could be described with τ_2 (**1**) = (20.3 ± 9.5) resp. τ_2 (**2**) = (19.0 ± 6.0) ps, *vs.* τ_2 (**3**) = (3.26 ± 0.85) ps. The very similar lifetimes strongly suggest that *trans–cis* isomerization of **1** and **2** after S_1 excitation is governed by the same mechanism. Since **1** cannot isomerize by a simple large-amplitude rotation of one of the phenyl rings about the central NN bond, the isomerization dynamics of both ABs should be better described as "inversion" at the N atom(s) rather than large-amplitude "rotation".

1. Introduction

The photo-induced *cis–trans* isomerization of azobenzene (AB) is of substantial interest for optical data-storage devices[1,2] or laser-triggered molecular switches.[3–8] However, the detailed mechanisms and dynamics of this prototypical reaction are still a matter of controversy. A longstanding question is whether the isomerization takes place as "inversion" on one of the N atoms or as large-amplitude "rotation" about the central NN bond or whether it requires more complex nuclear motions.[9,10]

Important experimental evidence pertaining to the ensuing reaction pathways has been reported by Rau and co-workers, who carried out quantum yield measurements for capped AB derivatives, in which a large-amplitude rotational motion of the aromatic rings during isomerization should not be feasible. In particular, they studied the photoisomerization of an azobenzophane[9] and the AB derivative **1**, in which the two aromatic rings are connected by a crown ether.[10] The experimental results were found to depend on whether the molecules were excited to the $S_1(n\pi^*)$ or to the $S_2(\pi\pi^*)$ electronic state. In particular, the quantum yields for isomerization of **1** and unsubstituted *trans*-AB (**3**) following excitation to the S_1 state were found to be practically the same within experimental error ($\Phi \approx 0.25$ and 0.29), while substantial differences ($\Phi \approx 0.11$ and 0.29, respectively) were encountered after excitation to the S_2 state.[10] Rau *et al.* thus concluded that S_1 excitation leads to isomerization by inversion, which they assumed to take place *via* a semi-linear planar CNNC transition state.

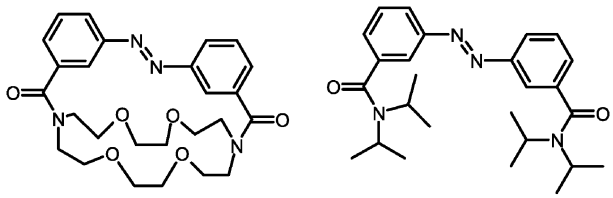

1 **2**

Transient absorption and fluorescence decay measurements carried out in the past few years showed that the isomerization of *trans*-AB after S_1 excitation takes place on time scales between a few hundred femtoseconds and several picoseconds.[11–16] The corresponding reaction of *cis*-AB has been found to be even faster.[15,16] Most workers assumed the above-mentioned semi-linear "inversion" pathway.[11–13,15] However, the "rotational" isomerization route has recently received substantial support from a number of quantum chemical calculations. In particular, calculations on the semi-linear inversion mechanism in the S_1 state predicted a potential energy barrier for that pathway.[14,17,18] In contrast, torsional motion has been suggested to lead to an easily accessible conical intersection (CI) between the S_1 and S_0 states that can mediate an ultrafast radiationless relaxation to the ground state near the 90° point of the CNNC out-of-plane rotation pathway.[17–20] In addition, Diau recently proposed a "concerted inversion" channel.[17] Chang *et al.* reported experimental evidence supporting the rotational isomerization route in low viscosity solvents (hexane) and the concerted inversion route in high viscosity solvents (ethylene glycol).[21] A time-resolved investigation of the photochemical dynamics of the capped

† Electronic supplementary information (ESI) available: Experimental details and crystal structure. See http://www.rsc.org/suppdata/cp/b4/b419236b/

DOI: 10.1039/b419236b

AB **1**, in which the rotational isomerization pathway does not appear possible, thus seems to be of great interest.

In this publication, we report on first results of a femtosecond time-resolved experimental study of the dynamics of *trans*-**1** (3,3′-bis(1,10-diaza-4,7,13,16-tetraoxa-18-crown-6-carbonyl)-*trans*-AB) and the chemically closely related open derivative *trans*-**2** (3,3′-bis(diisopropylaminocarbonyl)-*trans*-AB) in dioxane solution following excitation to the S_1 state. **1** has previously been studied with femtosecond time resolution only after excitation to the S_2 state at $\lambda = 303$ nm,[13] while **2** has not been investigated at all to our knowledge. The molecules were excited to the S_1 state at $\lambda = 475$ nm and the ensuing dynamics were monitored by femtosecond fluorescence up-conversion spectroscopy. A comparison of the results for the two AB derivatives with each other and with data for the parent compound *trans*-AB (**3**) provides some interesting new insight into the ensuing isomerization mechanisms.

2. Experimental section

Experiments were carried out at room temperature employing a flow sample cell with 0.2 mm sapphire windows and 1 mm optical path length.[16] Excitation light pulses at $\lambda = 475$ nm with ≈50 fs (Gaussian fwhm) duration were provided by a home-built non-collinear optical parametric amplifier (NOPA)[22] pumped by ≈200 μJ pulses from a regeneratively amplified Ti:sapphire femtosecond laser system (Clark MXR CPA 2001, $\lambda = 775$ nm, ≈150 fs fwhm, 1 kHz repetition rate). Excitation pulses of approximately 0.5 μJ were focused into the sample cell to a spot size of ≈400 μm. Fluorescence was collected and refocused into a 0.2 mm BBO crystal (GWU) for up-conversion by type II sum frequency generation with the 775 nm gate pulses (≈120 μJ) from the Ti:Sa laser using a pair of off-axis parabolic mirrors (Melles-Griot, $f = 119$ mm). A Schott OG550 filter between the mirrors removed scattered pump light. The upconverted light was bandpass filtered (Schott UG11), focused onto the entrance slit of an $f = 0.1$ m double monochromator (Jobin-Yvon HR 10), and detected with a photomultiplier (Hamamatsu R1527P) connected to a preamplifier (Stanford Research SR 445) and a gated photon counter (Stanford Research SR 400). Temporal fluorescence profiles were recorded by stepping the time delay of the gate pulses using a computer-controlled linear translation stage (Physik Instrumente M-126CG). The instrument response function (IRF), determined by upconverting scattered Raman light due to the CH stretching vibrations of the solvent or by cross correlation of the pump and gate pulses, was represented by a width parameter of $\tau_{irf} \approx 0.21$ ps (standard deviation of a normalized Gaussian, corresponding to a fwhm of ≈0.50 ps).

1 and **2** were synthesized as described in the electronic supplementary information (ESI)† following a modification of the procedure of Shinkai *et al.*[23] Both compounds (≈95 and 97% purity, respectively) were checked by NMR spectroscopy. Compound **1** was additionally characterized by single crystal X-ray diffraction.† The structure of **1** which is depicted in Fig. 1 confirmed the *trans* configuration of the azo moiety. In addition, it showed that the two aromatic rings are slightly non-coplanar (7°) and the aminocarbonyl groups are twisted by 58° with respect to the aromatic planes. The main impurity of **1** which could not be removed by simple means was the corresponding azoxybenzene. However, this molecule does not show any absorption at the excitation wavelength used[24] so that it does not affect the fluorescence measurements. Further details can be found in the ESI.†

Sample solutions were prepared using dry dioxane (Merck, Uvasol) and pumped through the cell using a peristaltic pump (Ismatec, MS-CA 2/860, 6.8 ml min^{-1} flow rate). The number of experimental runs that could be made was limited by the small amounts of substance available. Measurements of the poorly soluble **1** were carried out at a concentration of 5×10^{-4} M with ≈40 000 to 50 000 excitation pulses per time step. Five scans taken on different days were averaged to improve the signal-to-noise ratio. Measurements of **2** were carried out at a concentration of 1×10^{-3} M, resulting in a correspondingly higher signal-to-noise ratio, and two scans were averaged. *trans*-AB (**3**), purchased from Merck (98%), was measured at a concentration of 7.5×10^{-3} M.

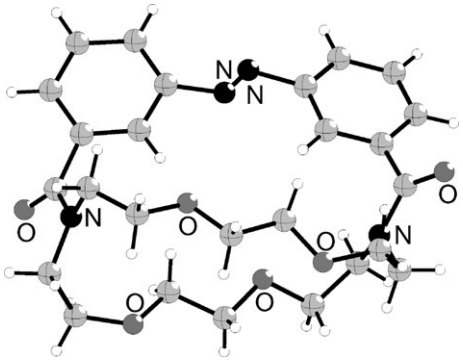

Fig. 1 X-Ray structure of **1**.

3. Results

3.1. UV absorption spectra

The investigations were initiated by measuring stationary UV/Vis spectra of the three molecules of interest. All three spectra are broad and unstructured. The weak first absorption maximum of *trans*-AB (**3**) is located at $\lambda = 445$–450 nm ($S_1 \leftarrow S_0$), the strong second transition peaks at $\lambda = 319$ nm ($S_2 \leftarrow S_0$).[24] A closer inspection suggests that the $S_1 \leftarrow S_0$ absorption maximum of *trans*-**1** may be slightly blue-shifted compared to *trans*-AB ($\Delta\lambda \approx 5$ nm), while the $S_2 \leftarrow S_0$ maximum appears red-shifted by about the same amount. The position of the $S_1 \leftarrow S_0$ band maximum of *trans*-**2** is virtually identical with that of *trans*-AB, while the $S_2 \leftarrow S_0$ maximum is slightly red shifted ($\Delta\lambda \leq 3$ nm). However, these differences are very minor. Thus, the *meta*-substitutions on the aromatic rings of the *trans*-AB nucleus by the aminocarbonyl groups and the crown ether appear to have little influence on the $n\pi^*$ and $\pi\pi^*$ excited electronic states of the AB moieties of the molecules. Significant differences between the UV spectra of **1** or **2** and the parent **3** were only observed at wavelengths of $\lambda \leq 280$ nm, where the derivatives exhibit additional absorption bands presumably due to the carbonyl groups, but this difference is not relevant in the present study of the S_1 state.

3.2. Time-resolved measurements

The $\lambda = 475$ nm pump pulses in the time-resolved experiments excited the molecules in the red wings of their $S_1 \leftarrow S_0$ absorption bands. Fluorescence was monitored at two detection wavelengths, $\lambda = 622$ and 655 nm, close to the peak of the emission spectrum of *trans*-AB.[14–16] Since the data taken at the two wavelengths did not show detectable differences they were averaged. The resulting temporal fluorescence profiles for the three molecules are displayed in Fig. 2. Although the data for **1** and **2** are somewhat noisy due to the poor solubilities and the limited number of experimental runs, it can be seen that the time profiles of the rotation-restricted capped AB **1** and the open derivative **2** are very similar. Both decay curves are biexponential, with two distinctive time constants. As can be clearly seen, the fluorescence from both derivatives decays more slowly than from the parent compound **3**.

For a quantitative analysis, the measured time profiles were fitted with a sum of two decaying exponentials convoluted with the IRF using a non-linear least-squares routine based on the Levenberg–Marquardt algorithm.[25] The two time constants

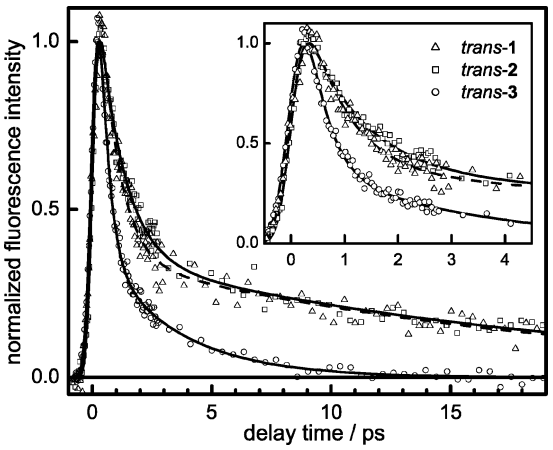

Fig. 2 Measured fluorescence decay curves of the *trans*-ABs **1**, **2**, and **3** in dioxane. The experimental data are given by the open symbols, the fitted profiles by the solid lines.

and two amplitudes were used as adjustable parameters. In addition, it was checked by varying τ_{irf} that the time resolution of the fluorescence measurements agreed with the IRF derived from the Raman signal and the pump-gate cross correlation. The fit results are collected in Table 1. The decay times of the first fluorescence components were found to be

$$\tau_1(\mathbf{1}) = 0.79 \text{ ps}, \tau_1(\mathbf{2}) = 1.05 \text{ ps}, \tau_1(\mathbf{3}) = 0.37 \text{ ps};$$

the second components were described with

$$\tau_2(\mathbf{1}) = 20.3 \text{ ps}, \tau_2(\mathbf{2}) = 19.0 \text{ ps}, \tau_2(\mathbf{3}) = 3.26 \text{ ps}.$$

4. Discussion

Considering the detailed molecular mechanisms responsible for the observed dynamics, we start with the following premises: (i) The observed ultrashort fluorescence lifetimes of *trans*-AB **3** and its derivatives **1** and **2** studied in the present work are related to ultrafast nonradiative electronic relaxation and *trans–cis* isomerization of the molecules. Both processes are assumed to take place through CIs between the S_1 and S_0 potential energy surfaces (PES) of the molecules near the mid-points of the *trans–cis* isomerization reaction coordinates.[11,14–21,26,27] As has been shown, S_1 fluorescence and excited state ($S_n \leftarrow S_1$) absorption decay on the same time scale and this decay is accompanied by the appearance of "hot" ground state absorption as signature of the $S_1 \rightarrow S_0$ internal conversion.[11,12,15,28] Thus, nonradiative electronic relaxation and isomerization of AB are closely connected. (ii) The measured $S_1 \rightarrow S_0$ absorption spectra do not indicate significant differences between the respective excited electronic state structures of the three molecules studied. This suggests that the initial states of the molecules after excitation to the S_1 PES should be comparable. (iii) The observed fast sub-picosecond to picosecond fluorescence decay times show that the *trans* → *cis* isomerization of AB is a barrierless or nearly barrierless reaction. (iv) The observed two fluorescence time scales (τ_1 and τ_2) are well separated, indicating that they should belong to two genuine dynamical processes.

In the following, we compare the fluorescence decay times of the three ABs of interest, consider work on related stilbenes, and discuss the dynamical processes which may be responsible for the observed two decay time scales.

Table 1 Fluorescence decay times and relative amplitudes for the rotation-restricted capped AB derivative **1**, the open derivative **2**, and the unsubstituted parent compound **3** in dioxane solution

trans-AB	a_1 (%)[a]	τ_1/fs[a]	a_2 (%)[a]	τ_2/fs[a]
1	75.3(95)	0.79(20)	24.7(56)	20.3(95)
2	72.2(61)	1.05(20)	27.8(51)	19.0(60)
3	79.7(74)	0.37(6)	20.3(39)	3.26(85)

[a] 2σ standard deviations in parentheses.

4.1. Observed fluorescence decay times

The striking result of the present work that sheds interesting light on the photoisomerization dynamics of ABs is that the temporal fluorescence decay profiles of the rotation-restricted capped AB **1** and the chemically similar open AB **2** are almost indistinguishable (*cf.* Fig. 2).

In particular, the fluorescence profiles of all three ABs studied exhibit distinctive biexponential decays. The "fast" fluorescence components (≈75% rel. amplitude) disappear on the sub-picosecond to picosecond time scale. The respective lifetimes of the derivatives **1** and **2** ($\tau_1 = 0.79$ and 1.05 ps) are only about 2.5 times longer than for the parent molecule **3** ($\tau_1 = 0.37$ ps). A larger difference (factor of six) between **1** and **2** on the one hand and **3** on the other was found for the "slow" fluorescence components (≈25% rel. amplitude); the observed lifetimes are $\tau_2 \approx 20$ ps for **1** and **2** *vs.* $\tau_2 \approx 3.3$ ps for **3**. Furthermore, the τ_1 value for **1** appears to be even slightly shorter than that for **2**, despite of the extra hindrance of the isomerization due to the crown ether, while the τ_2 values are virtually identical. The ratio of the fast and slow fluorescence amplitudes for all three ABs is $a_1/a_2 \approx 3/1$.

We note that it is by no means obvious whether the ultrafast kinetics of a barrierless or near barrierless reaction like the isomerization of AB (S_1) should follow a mono- or bi- or multi-exponential decay law. Dynamical models developed for the similar near barrierless excited state isomerization of *cis*-stilbene (*trans*-stilbene has a significant potential energy barrier for isomerization and is described by unimolecular rate theory[29]) indeed predicted non-exponential decays not attributed to two distinctive dynamical processes.[30] However, the experimental data on *cis*-stilbene available at the time showed mono-exponential behaviour.[30–32] The reported exponential decay time (≈1 ps) for *cis*-stilbene is significantly longer than that for *trans*- and *cis*-AB. Further, recent work showed that there is a shallow well on the excited *cis*-stilbene PES, supporting some low-frequency vibrations.[33,34] The *trans–cis* and *cis–trans* isomerization reactions of AB (S_1) thus appear to be much better prototypical examples for barrierless reactions than the *cis*-stilbene reaction.

In agreement with the literature on AB, we take the very clear separation between the observed two decay time scales (τ_1,τ_2) for AB and especially for the AB derivatives as evidence for (at least) two distinctive dynamical processes.[14,15,21,26,27] The striking similarities then strongly suggest that photoisomerization of the AB derivatives **1** and **2** is governed by the same molecular mechanisms. Whether or to which extent this also applies for the unsubstituted parent AB **3** remains a question which we defer to the end of this discussion. The comparison of the experimental decay times for the parent AB on the one hand and the derivatives on the other hand suggests that there are at least subtle differences.

4.2. Comparison with related stilbenes

As mentioned, the longstanding question is whether the reaction coordinate for the photoisomerization of AB is better characterized as "rotation" about the central NN bond or "inversion" at one (or both) of the N atoms. While the actual pathways may be more complex, a fundamental classification of the dynamics along these two lines is justified by comparison of the photoisomerization quantum yields of the cited capped ABs[9,10] (*e.g.*, **1**) and similar capped stilbenes. In particular,

Rau and Waldner recently reported that the photoisomerization quantum yield for a *trans*-stilbenophane is $\Phi = 0$.[35] This highly intriguing result is rationalized by the blocking of the "rotational" reaction coordinate in the stilbenophane.

For the case of stilbene and for several polyenes, it is well known that the *cis–trans* isomerization coordinate is much more complex than a simple large-amplitude rotation.[33,34] The actual isomerization coordinate for stilbene is assumed to be a mixture of several internal coordinates showing torsional motion around the ethylenic CC bond, including out-of-plane CH wag and other oscillatory motions on the multidimensional PES, which minimize solvent friction.[30,31] The term "hula-twist" motion has been coined to describe the combined effect.[33,34] However, the photoisomerization quantum yield of $\Phi = 0$ for the *trans*-stilbenophane shows that under the experimental conditions used neither rotation nor hula-twist nor inversion nor another type of motion appears to be a feasible reaction coordinate for that molecule.[35]

With these premises, the contrast between the photoisomerization quantum yield of $\Phi = 0$ for the stilbenophane[35] compared with the "normal" quantum yields found for the similar rotation-restricted azobenzophanes and the crown ether capped AB **1** ($\Phi \approx 0.24$ and 0.29)[10] can be rationalized only if the capped ABs undergo photoisomerization by "inversion". The same route is thus suggested for the open AB derivative **2**. The inversion may not take place *via* the originally proposed semi-linear CNNC configuration, for which there appears to be a potential energy barrier.[17,18] Instead, Diau proposed a concerted inversion pathway, *via* a CI between the S_1 and S_0 states at an almost linear CNNC configuration.[17] It is of interest in this context that according to a picosecond Raman study the NN bond of *trans*-AB in the S_1 state keeps a double bond character.[36] In addition, we would like to mention the possibility of a "hula-twist" reaction coordinate similar to the stilbene case, involving some out-of-plane motions of the N atoms as a "non-planar inversion" variant. The hula-twist motion, which has not yet been theoretically explored in sufficient detail, would lead to the same orientation of the phenyl ring as a planar inversion, whereas rotation of the phenyl group about the NN bond exchanges the C atoms on the two sides of the ring.

4.3. Mechanistic explanation of the bi-exponential decay profiles

Having identified inversion as the reaction pathway for the AB derivatives **1** and **2**, the origin of the biexponential decay curves moves into focus. Here, possible differences have to be taken into account between the dynamics of unsubstituted AB[15,21,27] and the AB derivatives. We shall discuss common features first and specific differences afterwards.

The starting point for the dynamics is defined by the location of the initial wavepacket prepared on the S_1 PES. Considering the $n\pi^*$ nature of the $S_1 \leftarrow S_0$ transition, where a non-bonding electron is removed from one of the N atom lone pairs, the Franck–Condon region is determined by a high degree of excitation of the S_1 NNC bending vibration. Incidentally, this vibration coincides basically with the inversion reaction coordinate. In addition, there is a shortening of the CN bond in the S_1 state compared to the S_0 state. The Franck–Condon determined initial location of the excited wavepackets on the S_1 PES at $t = 0$ should be similar for all three ABs.

In line with previous arguments,[15,21,27] the fast initial decay times ($0.3 \leq \tau_1 \leq 1$ ps, respectively) are therefore attributed to fast motion of the excited wavepackets on the S_1 PES away from the Franck–Condon region towards the CI (or CIs) with the S_0 PES. The direct motion leads the wavepacket along the steepest descent on the S_1 PES. The even faster ($\tau_1 \leq 0.1$ ps) decay of *cis*– compared to *trans*-AB is thus explained by a steeper gradient of the S_1 PES near the *cis* configuration.[15,16] At least initially, the wavepacket should move mainly along the NNC bending coordinate. This conclusion has been supported by a recent semiclassical dynamics calculation.[20] The longer τ_1 values of **1** and **2** compared to the parent molecule **3** are attributed to increased solvent friction due to the extended side chains. In addition, the direct wavepacket motion in the direction of steepest descent on the S_1 PES may be accompanied by some rapid partial intramolecular vibrational redistribution (IVR) among vibrational modes which are strongly coupled with the NNC bending mode. The molecules were prepared with about 2000–3000 cm^{-1} of internal energy above the S_1 origin, corresponding to several vibrational quanta which may be partially redistributed.

The slow fluorescence decay times of $\tau_2 \approx 20$ ps for the AB derivatives are attributed to their transition to the S_0 state through the CI along the inversion coordinate. This dynamics can be pictured as indirect, "diffusive" motion on the S_1 PES. The molecules may execute a sort of "meandering" motion, miss the CI on their first pass, and survive on the S_1 PES until they find the CI from different directions at a later time. The diffusive motion is partially a consequence of the fact that the CI is not located exactly on the initial direct path of the wavepacket and partially a consequence (and manifestation) of fast partial "IVR". Following Diau,[17] the CI between the S_1 and S_0 states is located along the concerted inversion coordinate at an almost linear CNNC configuration. The funneling of the wavepacket through the CI and the subsequent wavepacket evolution on the S_0 PES determine whether the product molecules end up in the *cis* or the *trans* configurations. The higher number of vibrational degrees of freedom and the increased solvent friction of the AB derivatives lead to a much slower "diffusive" arrival of the excited wavepacket at the CI, hence the increase of τ_2 from $\approx$3.3 ps to $\approx$20 ps with increasing molecular size. Additionally, on the time scale of $\approx$20 ps the molecules in the S_1 state experience substantial vibrational relaxation by the solvent. Thus, the τ_2 values for the derivatives are essentially attributed to vibrationally relaxed S_1 molecules. For the unsubstituted AB, τ_2 is too short for a large degree of vibrational relaxation within the S_1 state. Eventually, since the current experiments had to be optimized for parallel polarization detection to observe the extremely weak fluorescence from **1** and **2**, it cannot be excluded that rotational depolarization may play a small role.

Considering the unsubstituted parent *trans*- or *cis*-AB, the "inversion" mechanism has received support from Nägele *et al.* and Satzger *et al.*,[11,15,27] who compared time-resolved absorption results on *trans*- and *cis*-AB after S_1 ($n\pi^*$) and after S_2 ($\pi\pi^*$) excitation. Transient signals of *trans*-AB in ethanol or DMSO in the case of S_1 excitation were found to exhibit decay times of $\tau_1 \approx 0.3$ and $\tau_2 \approx$ 2–3 ps; those of *cis*-AB could be described with decay times of $\tau_1 \approx$ 0.1–0.17 and $\tau_2 \approx$ 0.9–1.0 ps, in excellent agreement with the fluorescence up-conversion data on the S_1 state obtained in our laboratory[16] and by Lu *et al.*[14] Apart from an additional very fast decay time ($\lesssim$0.1 ps) attributed to internal conversion from the S_2 to the S_1 state, virtually the same decay times were found following S_2 excitation, in agreement in this case with fluorescence up-conversion data by Fujino *et al.*[37] These results were interpreted by Satzger *et al.* in terms of a two step model, whereby an ultrafast radiationless transition ($\lesssim$0.1 ps) takes the molecules first from S_2 to S_1. The actual isomerization then follows from the subsequent large-amplitude motions on the S_1 PES towards the CI with the S_0 state close to the midpoint of the *cis–trans* isomerization coordinate. Further slow processes appearing on the 5–20 ps time scale were attributed to vibrational cooling of the produced hot ground state molecules. Likewise, Lednev *et al.*,[13] who reported transient absorption measurements of **1** after excitation to the S_2 state, found an exponential decay with

a lifetime of $\tau = 2.6$ ps, somewhat longer than the value of τ_1 found in the present work. In their case, the molecules were concluded to experience a fast internal conversion to the S_1 state within <0.5 ps. The differences between S_2 *vs.* S_1 excitation thus reflect the different starting positions of the dynamics of the wavepackets on the S_1 PES.

However, recent femtosecond fluorescence depolarization measurements of *trans*-AB excited to the S_1 state in solvents of different viscosity by Chang *et al.* showed that the dynamics of the prototypical parent AB is considerably more complex.[21] They observed that the fluorescence anisotropy of *trans*-AB in hexane decays with the same time constant as the slow fluorescence (τ_2). In contrast, the fluorescence anisotropy in ethylene glycol did not show a discernable decay. They concluded that both the rotation and the inversion routes are important, but that their relative contributions depend on the conditions. In low viscosity solvents (hexane) they assumed isomerization predominantly *via* out-of-plane CNNC torsional motion and the CI at the twisted configuration predicted by theoretical work,[17–20] while the concerted in-plane inversion pathway[17] was preferred in high-viscosity solvents (ethylene glycol). Quoted differences between the decay times and photoisomerization quantum yields of *trans*- *vs.* *cis*-AB and S_2 *vs.* S_1 excitation thus reflect different starting points of the excited wavepackets on the S_1 PES, different relative contributions of the rotation and inversion reaction pathways, and different branchings of the wavepackets into the *cis* or *trans* directions at the S_1–S_0 CIs.

5. Conclusions

In conclusion, we have studied the temporal fluorescence decay profiles of a rotation-restricted *trans*-AB derivative capped by a crown ether (**1**), a chemically similar open derivative (**2**), and the unsubstituted parent *trans*-AB (**3**) following excitation to the S_1 ($n\pi^*$) state. The observed biexponential fluorescence profiles for **1** and **2** were almost indistinguishable within experimental error, suggesting strongly that *trans–cis* isomerization of **1** and **2** after S_1 excitation is governed by the same mechanism. The results support the idea that the internal conversion and isomerization of the molecules proceeds through a conical intersection between the S_1 and S_0 states. The very fast first fluorescence decay time is attributed to the initial direct motion of the excited wavepacket on the S_1 PES away from the Franck–Condon region. The slower second fluorescence decay time is assigned to the transition from to the S_0 to the S_1 state by a slower, "diffusive" motion. The isomerization of the capped AB **1** and the open derivative **2** is concluded to proceed *via* a planar (and probably concerted) "inversion" at the N atom(s) or a type of "hula-twist" motion of the N atom(s) and phenyl ring(s). Further theoretical studies are needed to fully characterize the possible inversion routes.

Acknowledgements

The financial support of this work by the Deutsche Forschungsgemeinschaft and the Fonds der Chemischen Industrie is gratefully acknowledged. A.K. thanks the Fonds der Chemischen Industrie for a Liebig stipend, T.P. thanks the Fonds der Chemischen Industrie for a PhD fellowship.

References

1 T. Ikeda and O. Tsutsumi, *Science*, 1995, **268**, 1873.
2 Z. F. Liu, K. Hashimoto and A. Fujishima, *Nature*, 1990, **347**, 658.
3 I. Willner and S. Rubin, *Angew. Chem., Int. Ed.*, 1996, **35**, 367.
4 T. Hugel, N. B. Holland, A. Cattani, L. Moroder, M. Seitz and H. E. Gaub, *Science*, 2002, **296**, 1103.
5 N. B. Holland, T. Hugel, G. Neuert, A. Cattani-Scholz, C. Renner, D. Oesterhelt, L. Moroder, M. Seitz and H. E. Gaub, *Macromolecules*, 2003, **36**, 2015.
6 L. Ulysse, J. Cubillos and J. Chmielewski, *J. Am. Chem. Soc.*, 1995, **117**, 8466.
7 J. R. Kumita, O. S. Smart and G. A. Woolley, *Proc. Natl. Acad. Sci. USA*, 2000, **97**, 3803.
8 S. Spörlein, H. Carstens, H. Satzger, C. Renner, R. Behrendt, L. Moroder, P. Tavan, W. Zinth and J. Wachtveitl, *Proc. Natl. Acad. Sci. USA*, 2002, **99**, 7998.
9 H. Rau and E. Lüddecke, *J. Am. Chem. Soc.*, 1982, **104**, 1616.
10 H. Rau, *J. Photochem.*, 1984, **26**, 221.
11 T. Nägele, R. Hoche, W. Zinth and J. Wachtveitl, *Chem. Phys. Lett.*, 1997, **272**, 489.
12 I. K. Lednev, T.-Q. Ye, P. Matousek, M. Towrie, P. Foggi, F. V. R. Neuwahl, S. Umapathy, R. E. Hester and J. N. Moore, *Chem. Phys. Lett.*, 1998, **290**, 68.
13 I. K. Lednev, T.-Q. Ye, L. C. Abbott, R. E. Hester and J. N. Moore, *J. Phys. Chem. A*, 1998, **102**, 9161.
14 Y.-C. Lu, C.-W. Chang and E. W.-G. Diau, *J. Chin. Chem. Soc.*, 2002, **49**, 693.
15 H. Satzger, S. Spörlein, C. Root, J. Wachtveitl, W. Zinth and P. Gilch, *Chem. Phys. Lett.*, 2003, **372**, 216.
16 T. Pancur, PhD thesis, Christian-Albrechts-Universität zu Kiel, 2004.
17 E. W.-G. Diau, *J. Phys. Chem. A*, 2004, **108**, 950.
18 A. Cembran, F. Bernardi, M. Garavelli, L. Gagliardi and G. Orlandi, *J. Am. Chem. Soc.*, 2004, **126**, 3234.
19 T. Ishikawa, T. Noro and T. Shoda, *J. Chem. Phys.*, 2001, **115**, 7503.
20 C. Ciminelli, G. Granucci and M. Perisco, *Chem. Eur. J.*, 2004, 2327.
21 C.-W. Chang, Y.-C. Lu, T.-T. Wang and E. W.-G. Diau, *J. Am. Chem. Soc.*, 2004, **126**, 10109.
22 T. Wilhelm, J. Piel and E. Riedle, *Opt. Lett.*, 1997, **22**, 1494.
23 S. Shinkai, T. Nakaji, Y. Nishida, T. Ogawa and O. Manabe, *J. Am. Chem. Soc.*, 1980, **102**, 5860.
24 H.-H. Perkampus, *UV-Vis Atlas of Organic Compounds*, VCH, Weinheim, 2nd edn., 1992, vol. 1.
25 W. H. Press, B. P. Flannery, S. A. Teukolsky and W. T. Vetterling, *Numerical Recipes in C*, Cambridge University Press, Cambridge, 1988.
26 T. Schultz, J. Quenneville, B. Levine, A. Toniolo, T. J. Martinez, S. Lochbrunner, M. Schmitt, J. P. Shaffer, M. Z. Zgierski and A. Stolow, *J. Am. Chem. Soc.*, 2003, **125**, 8098.
27 H. Satzger, C. Root and M. Braun, *J. Phys. Chem. A*, 2004, **108**, 6265.
28 P. Hamm, S. Ohline and W. Zinth, *J. Chem. Phys.*, 1997, **106**, 519.
29 J. Schroeder, T. Steinel and J. Troe, *J. Phys. Chem. A*, 2002, **106**, 5510.
30 D. C. Todd, J. M. Jean, S. J. Rosenthal, A. J. Ruggiero, D. Yang and G. R. Fleming, *J. Chem. Phys.*, 1990, **93**, 8658.
31 A. Abrash, S. Repinec and R. M. Hochstrasser, *J. Chem. Phys.*, 1990, **93**, 1041.
32 L. Nikowa, D. Schwarzer, J. Troe and J. Schroeder, *J. Chem. Phys.*, 1992, **97**, 4827.
33 K. Ishii, S. Takeuchi and T. Tahara, *Chem. Phys. Lett.*, 2004, **398**, 400.
34 W. Fuß, C. Kosmidis, W. E. Schmid and S. A. Trushin, *Chem. Phys. Lett.*, 2004, **385**, 423.
35 H. Rau and I. Waldner, *Phys. Chem. Chem. Phys.*, 2002, **4**, 1776.
36 T. Fujino and T. Tahara, *J. Phys. Chem. A*, 2000, **104**, 4203.
37 T. Fujino, S. Y. Arzhantsev and T. Tahara, *J. Phys. Chem. A*, 2001, **105**, 8123.